Batteries & Supercaps

Review
doi.org/10.1002/batt.202400237

Chemistry Europe
European Chemical Societies Publishing

www.batteries-supercaps.org

Electrolyte Stabilizes Zn^{2+} Reduction Reaction Process: Solvation, Interface and Kinetics

Yan Xu,[a] Zhaohe Guo,[a] Ming Song,*[a] Xuena Xu,[b] Hongri Wan,[a] Limei Sun,[a] Dongliang Chao,[c] and Wanhai Zhou*[c]

Aqueous zinc-ion batteries (ZIBs), lauded for their low cost, eco-friendliness, and high safety, have garnered significant attention. However, their commercial viability is hindered by the challenges of dendrite growth and side reactions during the Zn^{2+} reduction reaction process. Electrolyte as the indispensable component of batteries has a close relationship with the issues mentioned above. With the feature of simplicity, effectiveness, and scalability, regulating electrolytes is a particularly promising, feasible, and straightforward approach to stabilizing the Zn anode. The solvation design with less solvated water, interface optimization with water-poor and pH-stable interface, and kinetics regulation with fast Zn^{2+} transport, uniform Zn^{2+} flux, and orientational Zn growth can contribute to uniform Zn deposition with restrained corrosion. This review encapsulates the cutting-edge advancements in electrolytes to stabilize the Zn anode. The mechanisms underlying these advancements, encompassing solvation structure design, Zn-electrolyte interface optimization, and kinetics regulation are elucidated. Finally, this paper outlines current challenges and prospects in electrolyte development for ZIBs, providing valuable insights for future endeavors in this field.

1. Introduction

Energy is an indispensable element for the continuous advancement of human society. In light of dwindling fossil fuel reserves and escalating environmental concerns, the rapid development of abundant and eco-friendly renewable energy sources such as wind, solar, and tidal energy has been witnessed in recent years.[1] However, these renewable energies, which are constrained by their indirect nature and geographical limitations, cannot be directly integrated into the power grid without potentially destabilizing the stability of the electric energy storage system.[2] Thus, it is urgent to develop highly efficient energy storage systems to ensure the sustainable utilization of renewable energies.[3]

Electrochemical batteries have emerged as efficient technologies for the conversion and storage of electrical energy. Lithium-ion batteries (LIBs), characterized by their lightweight design and high energy density, have found widespread applications across various domains, currently dominating the battery market.[4] Nevertheless, LIBs face limitations in applications such as smart wearable devices and large-scale energy storage systems because of the safety concerns, resource constraints, and cost issues.[5] Aqueous Zinc-ion batteries (ZIBs) with high safety, abundant resources, low costs, non-toxicity, and ease of manufacturing, have garnered considerable attention in recent years.[6] Moreover, ZIBs with aqueous electrolytes have the high theoretical capacity (802 mAh g^{-1} or 5855 mAh cm^{-3}),[7] rational redox potential (−0.76 V vs. standard hydrogen electrode),[8] and high ionic conductivity (10~100 mS cm^{-1}),[9] exhibiting immense potential in smart wearables and grid-scale energy storage systems.

In recent years, significant efforts have been spent on improving the cathode performance of ZIBs. Numerous novel materials, including vanadium-based materials, manganese-based materials, and Prussian blue analogues, have been developed, yielding significant breakthroughs.[10] However, challenges persist with the Zn anode in ZIBs, such as Zn dendrite and side reactions.[11] These issues can lead to irreversible capacity degradation and battery failure, thereby impeding the commercial application of ZIBs.[12] Various strategies have been proposed to cope with these challenges, which can be categorized into three types: constructing special structures,[13] modifying the separator,[14] and developing novel electrolytes.[15] Among these strategies, electrolyte engineering stands out for its simplicity, effectiveness, and scalability.[16] Tuning the kind and concentration of electrolyte is a powerful strategy to improve the performance of Zn-based batteries.[17] In addition, electrolyte is also crucial for ZIBs in extreme conditions, such as low temperature and high temperature. As the solvent of ZIBs is based on water, the physicochemical properties below 0 °C can result in the reduced ionic conductivity, the poor electrolyte-electrode wettability, and the electrolyte solidification. When the temperature exceeds to 40 °C, the solvent evaporation, solute precipitation may occur.[18] More importantly, the low temperature may render deteriorative dendrites growth, while the high temperature can cause

[a] Y. Xu, Z. Guo, Prof. M. Song, H. Wan, L. Sun
School of Materials and Chemical Engineering, Xuzhou University of Technology, Xuzhou 221018, China
E-mail: mings@xzit.edu.cn

[b] X. Xu
Department of Mechanical Engineering, Tsinghua University, Beijing 100084, China

[c] Prof. D. Chao, Prof. W. Zhou
Laboratory of Advanced Materials, Shanghai Key Laboratory of Molecular Catalysis and Innovative Materials, Fudan University, Shanghai, 200433, China
E-mail: zhouwh@fudan.edu.cn

aggravating side reactions.[19] Due to the importance of electrolyte for the ZIBs, this review aims to provide a timely update on recent progress in electrolyte strategies for enhancing Zn anode stability. It begins by outlining the challenges associated with the Zn anode, followed by a detailed discussion of various electrolyte strategies to stabilize the Zn^{2+} reduction reaction process. Finally, a summary and outlook is presented, hoping that this timely review of electrolyte strategies for ZIBs can offer valuable insights for future development.

2. Issues in Zn Anodes

2.1 Zn Dendrite

Similar to the lithium metal anode, the Zn anode is plagued by Zn dendrite, which is a concern particularly pronounced under extreme conditions such as high capacity and current density. Notably, Zn dendrites possess greater hardness than lithium dendrites, rendering them more prone to puncturing the separator and inducing short circuits. The large current can also increase the probability of " soft shorts" in ZIBs.[20] Additionally, the detachment of Zn dendrites or protrusions from the Zn electrode may lose their capacities[21] and result in the formation of "dead Zn", leading to diminished Coulombic Efficiency (CE). Consequently, Zn dendrite is one of the foremost challenges hindering the practical application of ZIBs.[3]

In neutral or slightly acidic electrolytes, Zn^{2+} can undergo direct reduction on the Zn anode, with uneven Zn deposition serving as the inducement for dendrite formation. The process of Zn dendrite formation can be delineated into two stages: Zn nucleation and Zn growth. Zn nucleation is intricately linked with the nucleation overpotential, signifying the barrier to nucleation. The impetus to surmount this barrier is derived from the electrical field, ion concentration, and surface energy, all of which are contingent upon the surface of electrode.[8a] Irregular and non-ideal Zn surface can engender disparate distributions of electrons and ions, thereby fostering uneven Zn nucleation.[9c] The uneven distribution of Zn nuclei may exacerbate the non-uniform electric field, prompting Zn atoms to preferentially accumulate at existing tips to minimize surface energy, thereby fostering dendrite growth.

2.2 Side Reactions

2.2.1 Hydrogen Evolution

Typically, Zn^{2+} is coordinated with six water molecules, forming $Zn[H_2O]_6^{2+}$ complexes in the aqueous electrolyte. Coordinated water molecules can convert into "active water", facilitating the production of H_2 through the hydrogen evolution reaction (HER) during the Zn deposition process. As illustrated in Equation (1) and (2),[22] the favorable thermodynamics make HER easy occurrence. However, Zn deposition precedes HER owing to the sluggish kinetics of the latter.[2] In practice, the polar potential during Zn deposition may still instigate HER, reducing the CE. The resultant H_2 generation would elevate the internal pressure of the battery, causing battery deformation and bulge. Furthermore, the depletion of protons can lead to localized pH elevation, resulting in the formation of by-products. Depending on the electrolyte and the amount of active water, the by-products will also be different. $Zn_4(OH)_6SO_4 \cdot xH_2O$ as depicted in Equation (3) will form in $ZnSO_4$ electrolyte during the discharging process.[2] In the $Zn(CF_3SO_3)_2$ electrolyte, the product will be $Zn_m(OH)_{2m-n}(CF_3SO_3)_n \cdot xH_2O$,[23] while $Zn_5(OH)_8Cl_2 \cdot xH_2O$ will form in $ZnCl_2$ electrolyte.[24] The by-product composed of Zn^{2+} ions, OH^-, anions and water molecules, can be expressed as $(Zn(OH)_y(anion)_z^{+1/+2} \cdot xH_2O)$.[25] These by-products may passivate the Zn surface and impair battery performance.

Zn deposition:

Yan Xu is presently working at Xuzhou University of Technology. She received her Ph.D. in Chemical Engineering and Technology from Sichuan University in 2014. She is currently an associate professor and her research interests focus on electrochemical functional materials and novel electrolytes for storage batteries.

Ming Song received his Ph.D. from Sichuan University in 2014. He is currently an associate professor at Xuzhou University of Technology and serving as Academic Vice Dean of School of Materials and Chemical Engineering. His research interests focus on electrochemical functional materials and energy storage systems. He is ranked as one of the World's Top 2% most-cited scientists for 2023 by Stanford University.

Wanhai Zhou is an associate professor at the Laboratory of Advanced Materials, Fudan University. He received his PhD degree from Sichuan University in 2020. He worked as a postdoctor at Fudan University in 2021–2023 under the direction of Prof. Dongyuan Zhao. His current research focuses on energy materials and battery devices, including zinc, tin, and sulfur-based aqueous batteries, and sodium-ion batteries.

$$Zn^{2+} + 2e^- \leftrightarrow Zn, E^0 = -0.76 Vvs.SHE \quad (1)$$

Hydrogen evolution reaction (HER):

$$2H^+ + 2e^- \leftrightarrow H_2, E^0 = 0 Vvs.SHE \quad (2)$$

By-product formation ($ZnSO_4$ electrolyte):

$$3Zn^{2+} + 6OH^- + ZnSO_4 + xH_2O \leftrightarrow ZnSO_4[Zn(OH)_2]_3 \cdot xH_2O \quad (3)$$

2.2.2 Zinc Corrosion

Zinc corrosion, as depicted in Equation (4), can also result in detrimental effects. Zinc corrosion encompasses spontaneous chemical corrosion and electrochemical corrosion. The electrochemical corrosion stems from impurities and zinc, resembling microscale galvanic batteries.

$$Zn + 2H^+ \leftrightarrow Zn^{2+} + H_2 \uparrow \quad (4)$$

In ZIBs, the aforementioned issues exist a close interrelation, as depicted in Figure 1.[3,16] Uneven Zn surfaces can precipitate the formation of Zn dendrite, consequently increasing the available surface area. Subsequently, a larger portion of Zn metal becomes susceptible to electrochemical corrosion, leading to the formation of $ZnSO_4[Zn(OH)_2]_3 \cdot xH_2O$. This, in turn, necessitates a higher polar potential, thereby accelerating the occurrence of HER. Following this, the proliferation of rough Zn surfaces further promotes the growth of Zn dendrites. From another point of view, the smooth surface may homogenize Zn nucleation and growth, however, it also serves as a reactive contact area for parasitic reactions, culminating in HER.[26]

Electrolyte which is an indispensable component of ZIBs can serve as a transport medium. It plays a crucial role in Zn^{2+} reduction reaction process. For example, the ion concentration can affect the formation of Zn dendrite, the active water can induce HER, and the elevation of pH can lead to the generation of by-products. Therefore, achieving a stable Zn anode necessitates the design of multifunctional electrolytes by researchers.

3. Electrolyte Strategies to Stabilize Zn Anodes

3.1 Design of Solvation Structure

In aqueous electrolytes, a stable sheath-like structure forms among cations/anions, additives, and solvents, known as the solvation structure. Metal cations, particularly Zn^{2+}, exhibit a strong tendency to combine with water molecules to form hydrated metal ions. Due to its bivalent nature, Zn^{2+} induces strong interactions with surrounding electron donors, resulting in the formation of $Zn[H_2O]_6^{2+}$. Notably, the absence of hydrogen bonds between coordinated H_2O molecules and the electrode/electrolyte interface renders these H_2O molecules active, predisposing them to proton shedding and inducing undesired side reactions.[8b] Hence, the solvation structure of Zn^{2+} can be changed by reducing water content or introducing other ligands with high electron-donor numbers (Figure 2a).[27]

Researchers have proposed a high-salt-concentration strategy, termed the water-in-salt electrolyte, where high salt concentrations induce water-starved conditions.[28] In such conditions, anions can infiltrate the solvation sheath structure, modifying the solvation structure of Zn^{2+}.[15c] For instance, Wang and colleagues investigated a LiTFSI-based electrolyte (1 m $Zn(TFSI)_2$ + 20 m LiTFSI) for ZIBs, demonstrating that Zn^{2+} was enveloped by $TFSI^-$ rather than water when LiTFSI concentrations exceeded 20 m. The formation of $Zn[TFSI]^+$ effectively suppressed the formation of $Zn[H_2O]_6^{2+}$, thereby mitigating H_2 evolution and enabling dendrite-free Zn plating.[29] Similarly, various electrolytes such as 30 m $ZnCl_2$,[30] 1 m $Zn(OTf)_2$ + 20 m LiTFSI,[31] 30 m KOAc + 3 m LiOAc + 3 m $Zn(OAc)_2$,[32] 0.5 m $Zn(ClO_4)_2$ + 18 m $NaClO_4$,[33] and 30 m $ZnCl_2$–water solution + ACN (3 : 1)[34] have demonstrated excep-

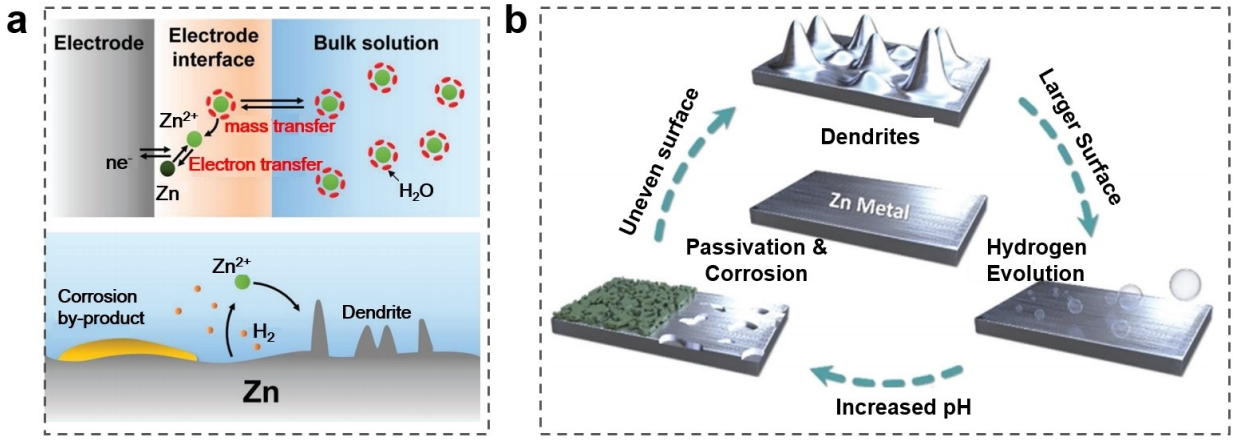

Figure 1. Issues in Zn anode. (a) Schematics of the plating-stripping process and the problems of Zn anode in a mild electrolyte. Reproduced with permission from Ref. [16]. Copyright 2023 John Wiley and Sons. (b) The relationship among the problems in Zn anode. Reproduced with permission from Ref. [3]. Copyright 2023 John Wiley and Sons.

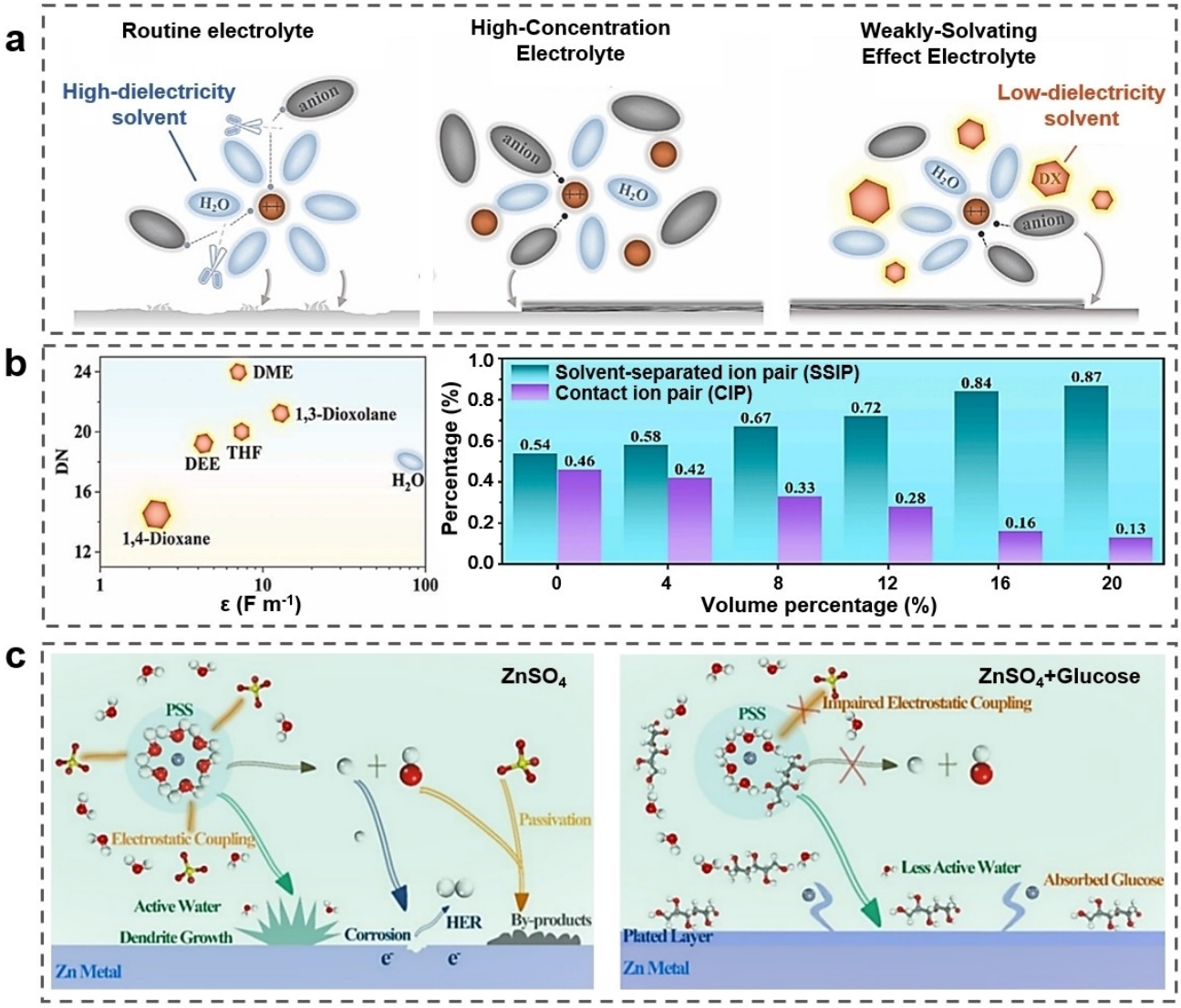

Figure 2. Modification of solvation structure of Zn^{2+}. (a) Schematic illustrations of the solution structures for the solvation structure of Zn^{2+}. Reproduced with permission from Ref. [38]. Copyright 2023 John Wiley and Sons. (b) The diagram for permittivity and DN of solvents towards Zn^{2+}, and the ratio of SSIP to CIP with increasing ETH content. Reproduced with permission from Ref. [39]. Copyright 2024 Elsevier. (c) Schemes illustrating different reaction processes of Zn^{2+} solvation structure and corresponding interfacial interaction between Zn anode surface and electrolyte. Reproduced with permission from Ref. [43]. Copyright 2021 John Wiley and Sons.

tional performance in ZIBs. However, the extensive use of salt in electrolytes may introduce other issues, such as counteracting the cost advantages of aqueous electrolytes, decreasing ionic conductivity due to increased viscosity, and so on.

Eutectic electrolytes containing low percentage of water molecules have also been proven effective in preventing side reactions induced by water molecules. In hydrated eutectic electrolytes (e.g. $Zn(OTf)_2$ + tetramethylene sulfone (TMS) + H_2O), the activity of H_2O is decreased by forming hydrogen bonds between TMS and H_2O in the solvation of Zn^{2+}. Furthermore, the primary solvation shell of Zn^{2+}–$6H_2O$ can be modulated by TMS, ultimately achieving a novel solvent co-intercalation mechanism ($[Zn–TMS]^{2+}$).[35] Ma et al. studied the electrolytes containing $Zn(BF_4)_2$, acetamide (ace), and water. They revealed that a significant increase in water content could disrupt the eutectic system, resulting in Zn corrosion.[36] A quaternary hydrated eutectic electrolyte with a ligand-cation-anion cluster $[ZnCl_{1.4}(ACA)_{1.7}(HDO)_{0.9}(H_2O)_2]$ was also reported, and the hydration-deficient complexes induced by competing eutectics and water molecules confined the free water activity.[37]

The solvating power of solvents can be quantified by dielectric constant and electron-donor number, which can influence the electrostatic force and the nucleophilic behavior, respectively.[6a,38] Based on this, weakly solvating electrolytes have been developed to regulate the solvation structure of Zn^{2+}. Ethanol (ETH) was employed to construct a low-dielectric aqueous electrolyte. The coordination environment of Zn^{2+} was modulated and the proportion of solvent-separated ion pairs ($Zn^{2+}(H_2O)_6SO_4^{2-}$) was increased with increasing ETH content (Figure 2b).[39] Lu et al. reported an H_2O-poor solvation structure of Zn^{2+} by introducing low-dielectric-constant acetone to the

electrolyte. It reduced the solvating power of H_2O and allowed OTF^- to enter the primary solvation sheath of Zn^{2+}, thereby decreasing the number of solvated H_2O.[40] The dimethyl sulfoxide (DMSO) with a higher gutmann donor number than H_2O was also added to the diluted aqueous electrolytes, suppressing the side reactions.[41]

Additionally, low-cost additives can also manipulate the solvation structure of Zn^{2+}. If the interaction between Zn^{2+} and the additive is stronger than that between Zn^{2+} and H_2O, the additive molecule can enter the solvation structure of Zn^{2+} and replace coordinated H_2O.[42] For instance, Sun et al. found that glucose could modulate the solvation structure of Zn^{2+} in the $ZnSO_4$ electrolyte, effectively suppressing by-reaction derived from active water around the Zn anode (Figure 2c).[43] Huang et al. discovered that gamma butyrolactone (GBL) could decrease the bonding strength of Zn^{2+}-coordinated H_2O in the $ZnSO_4$ electrolyte, reducing water activity and suppressing side reactions.[44] Moreover, additives such as carboxymethyl cellulose (CMC), penta–sodium diethylene–triaminepentaacetic acid salt (DTPA–Na), and gum Arabic (GA) were also applied to modulate the Zn^{2+} solvation sheath to stabilize the Zn anodes.[45]

In addition, regulating the electrolyte solvation structure and reconstructing the hydrogen bonds network of H_2O can also contribute to the high performance ZIBs at wide-temperatures. Liu et al. found that the trimethyl phosphate (TMP) could reshape the Zn^{2+} solvation structure. The Zn||VO_2 full cell exhibited an ultralong cyclic performance at 0 °C.[46] Xie et al reported that the weak solvent (γ-valerolactone) could act as a strong hydrogen bonds ligand and break the hydrogen bonds between free H_2O molecules, enhancing the temperature tolerance of batteries. The symmetric cell delivered an excellent stability at the temperature range of −50 to 80 °C.[47] Acetamide (AC) which could disrupt the original hydrogen bonds network of H_2O and replace the solvated H_2O in Zn^{2+} solvation structure was also reported to be an effective additive for ZIBs to achieve a long-term lifespan across −20–60 °C.[48]

3.2 Optimization of Zn–Electrolyte Interface

The electrode-electrolyte interface is crucial for the Zn^{2+} reduction reaction process. Optimizing the Zn–electrolyte interface, such as constructing molecular sieve membrane[49] and protection layer[50] can reduce the water activity and side-reaction. In particular, the interface constitutes an electric double layer (EDL), which encompasses the diffusion layer, outer Helmholtz plane (OHP), and inner Helmholtz plane (IHP). The IHP is delineated by the charge centers of adsorbed water molecules, where both parasitic reactions and battery reactions occur (Figure 3).[51] During the Zn deposition process, the de-solvation of $Zn[H_2O]_6^{2+}$ can lead to excess active water on the IHP, instigating undesirable side reactions. Moreover, the Zn–electrolyte interface profoundly influences Zn nucleation and Zn^{2+} diffusion, which is intimately linked with the formation of Zn dendrite. Consequently, stabilizing the Zn

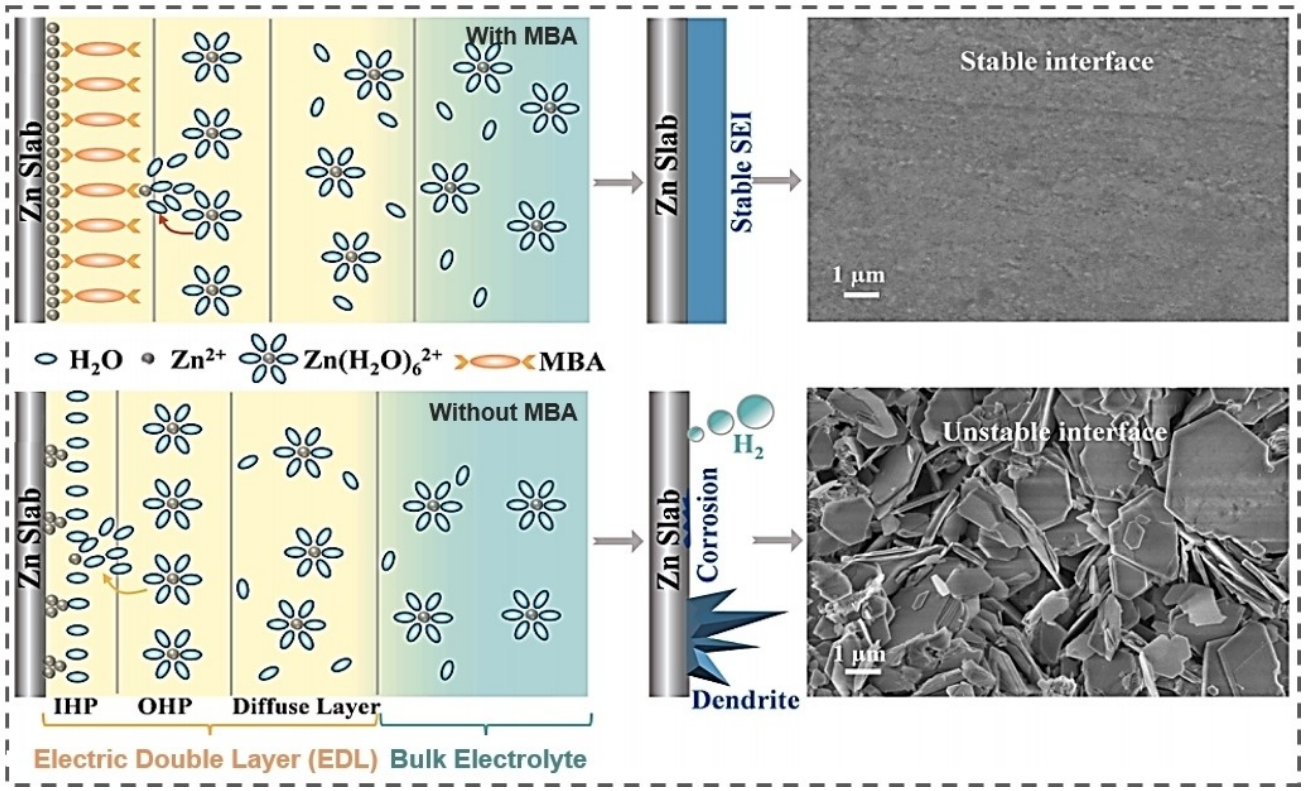

Figure 3. Schematic of the EDL structure in the electrolyte with or without N,N′–Methylenebisacrylamide (MBA). Reproduced with permission from Ref. [51]. Copyright 2024 Elsevier.

anode necessitates the optimization of Zn–electrolyte interface, including artificial (or derived) solid electrolyte interphase (SEI) construction, Helmholtz plane reconstruction, active site blocking, and pH stabilization.[52]

The SEI layer can be facilely constructed by proper electrolyte additives. During cycling, some additives may decompose on the surface of Zn anode, yielding salts that can serve as the SEI layer.[53] For instance, Ouyang et al. employed carboxymethylcellulose sodium (CMC–Na) in $ZnSO_4$ electrolyte. Initially, CMC^- aggregated on the Zn surface, generating an H_2O-poor and CMC^--rich EDL. Then, partial CMC^- decomposed, forming a unique SEI during cycling. The SEI was beneficial for regulating Zn^{2+} deposition behavior, resulting in the dendrite inhibition and by-product limitation.[54] Similarly, the silk fibroin (SF) molecules could adsorb on the surface of the Zn anode, forming a protective film as depicted in Figure 4. The film exhibited strong Zn^{2+} ion affinity, promoting the homogeneous Zn deposition, while its excellent insulating behavior effectively suppresses parasitic reactions.[55] Additionally, tris(2,2,2-trifluoroethyl)phosphate (TTFEP) with abundant C–F functional groups could attach onto the Zn surface, forming a fluorinated interphase layer.[56] Dioxane with two oxygen sites had an affinity for Zn and Zn^{2+}, and could form a stable SEI upon adsorption onto the Zn surface, suppressing HER and promoting homogenized Zn deposition.[57] In addition, the byproduct of $Zn_4(OH)_6SO_4 \cdot xH_2O$ on Zn electrode could also serve as the SEI to restrain the dendrites and side reactions by introducing a small amount of $Zn(OH)_2$ into the $ZnSO_4$ electrolyte.[58] Other substances such as ionic liquid and penta–potassium triphosphate were also able to form in-situ SEI layer on the Zn surface.[59]

The robust adsorption of additives on the Zn anode also has the capability to modify the Helmholtz plane. Hu et al. reconstructed the Helmholtz plane by using zinc pyrrolidone carboxylate (PCA–Zn) as an additive to the $ZnSO_4$ electrolyte. They posited that the dissociated PCA^- with electron-rich bis-

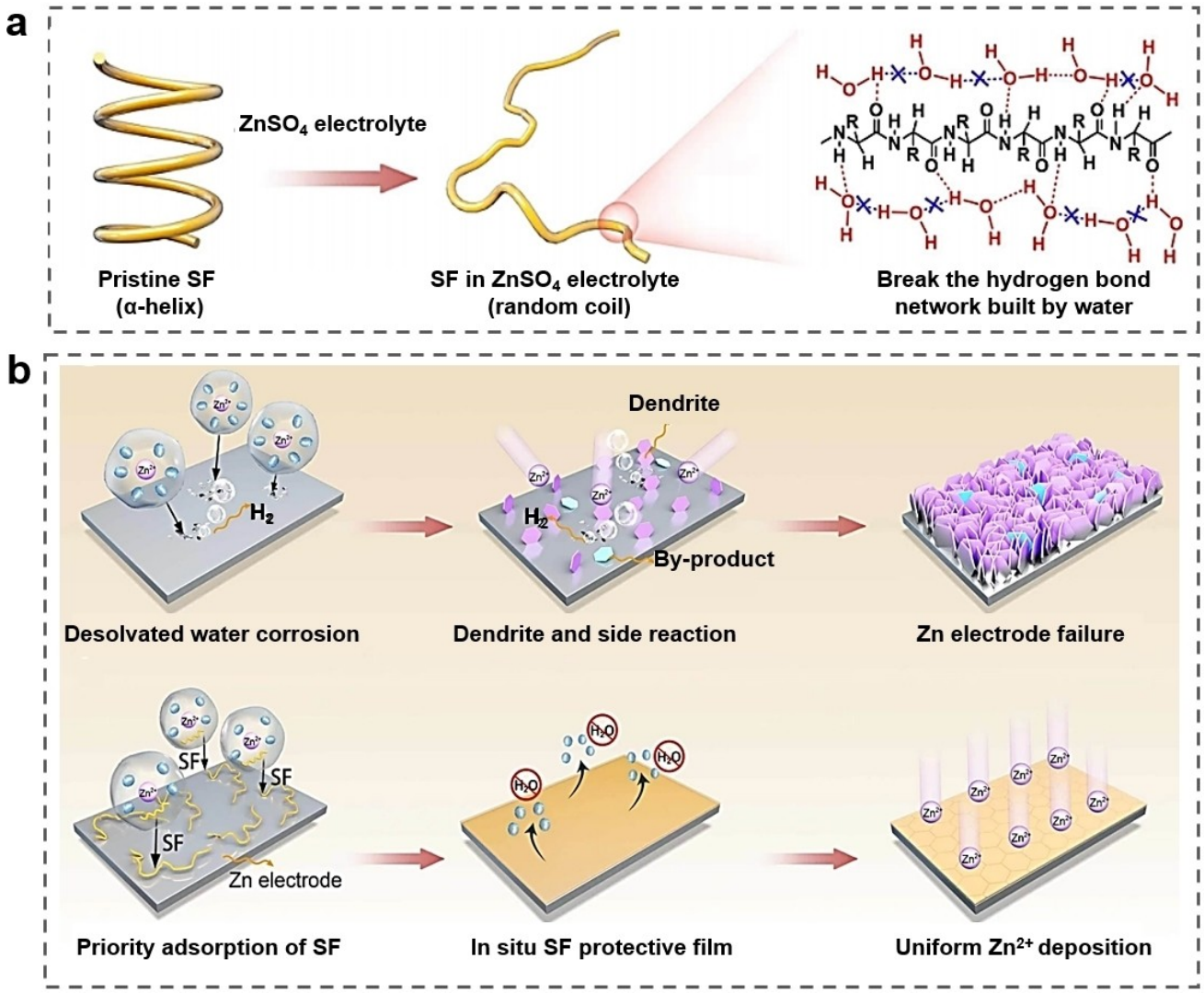

Figure 4. Formation of SEI on the interface of Zn–electrolyte. (a) Illustration of the secondary structural transformation of SF molecules and the breaking of the hydrogen bond network between water molecules. (b) Illustration of the morphology transition on Zn anode surface in $ZnSO_4$ electrolyte with and without SF additive. Reproduced with permission from Ref. [55]. Copyright 2022 American Chemical Society.

terminals exhibited a pronounced affinity to the Zn anode. The preferential adsorption of PCA^- on Zn anode could result in the reconstruction of the Helmholtz plane containing zincophilic species. In the electroplating process, Zn^{2+} tended to deposit on the protrusions of the Zn anode in bare $ZnSO_4$ electrolyte. Conversely, in the electrolyte containing PCA–Zn, Zn^{2+} underwent desolvation subsequent to traversing the adsorbed PCA^- layer. The coordinated water molecules were sequestered outside the PCA^- layer, as illustrated in Figure 5a. Due to the shielding effect against H_2O/SO_4^{2-} species and spatial confinement of Zn^{2+}, the water-induced side reactions and the uncontrolled diffusion of Zn^{2+} were suppressed.[60] Xu et al. introduced tranexamic acid (TXA) to $ZnSO_4$. The TXA with $-NH_2$ and –COOH groups exhibited a higher adsorption energy than H_2O on Zn metal, thus, it facilitated the reconfiguration of the Zn–electrolyte interface. The resulting H_2O-poor interface impeded direct contact between Zn and H_2O, thereby suppressing side reactions (Figure 5b).[61] Urea, possessing one carbonyl group and two amino groups, was found to adsorb onto the Zn surface, forming a stabilized self-assembled organic layer. This layer effectively prevented water from contacting the Zn anode directly, and facilitated the 3D diffusion of Zn^{2+}, consequently inhibiting dendrite formation and side reactions (Figure 5c).[62] Besides, the gluconate anions exhibited a preference for horizontal adsorption on metallic Zn. It could shield protrusions and fill concavities, resulting in a dendrite-free Zn deposition.[63] Glutamine (Gln) was capable of constructing a water-poor interface.[64] Hexamethylenetetramine (HMTA) could establish an anode-molecule interface.[65] Succinimide (SI) had the capacity to occupy and compact the EDL and protect the Zn anode from corrosion.[66] Glycine could reduce the EDL repulsive force of Zn^{2+} and isolate H_2O from the anode surface, and it also enabled superior electrochemical performance in a wide range of temperature (−15–50 °C).[67]

HER may occur during the Zn deposition process, increasing the pH. The local increased pH can lead to the generation of inert by-products with loosely packed plate-like morphology on the Zn–electrolyte interface. Consequently, these by-products can induce nonuniform zinc ion flux, giving rise to the generation of Zn dendrites.[68] Researchers have found that adding additives could stabilize the pH of the electrolyte, inhibiting side reactions. For example, Pan et al. utilized $(NH_4)_2S_2O_8$ to regulate the pH of $ZnSO_4$ electrolyte. NH^{4+} and $S_2O_8^{2-}$ could function as pH buffers, dynamically adjusting the concentrations of H^+ and OH^- at the interface, thereby suppressing the HER and the generation of by-products (Figure 6a). The pH evolution of the electrolyte with and without $(NH_4)_2S_2O_8$ was illustrated in Figure 6b.[69] Yang et al. demonstrated that N–methylimidazole (NMI) additive could effectively remove OH^- from the Zn–electrolyte interface, suppressing the

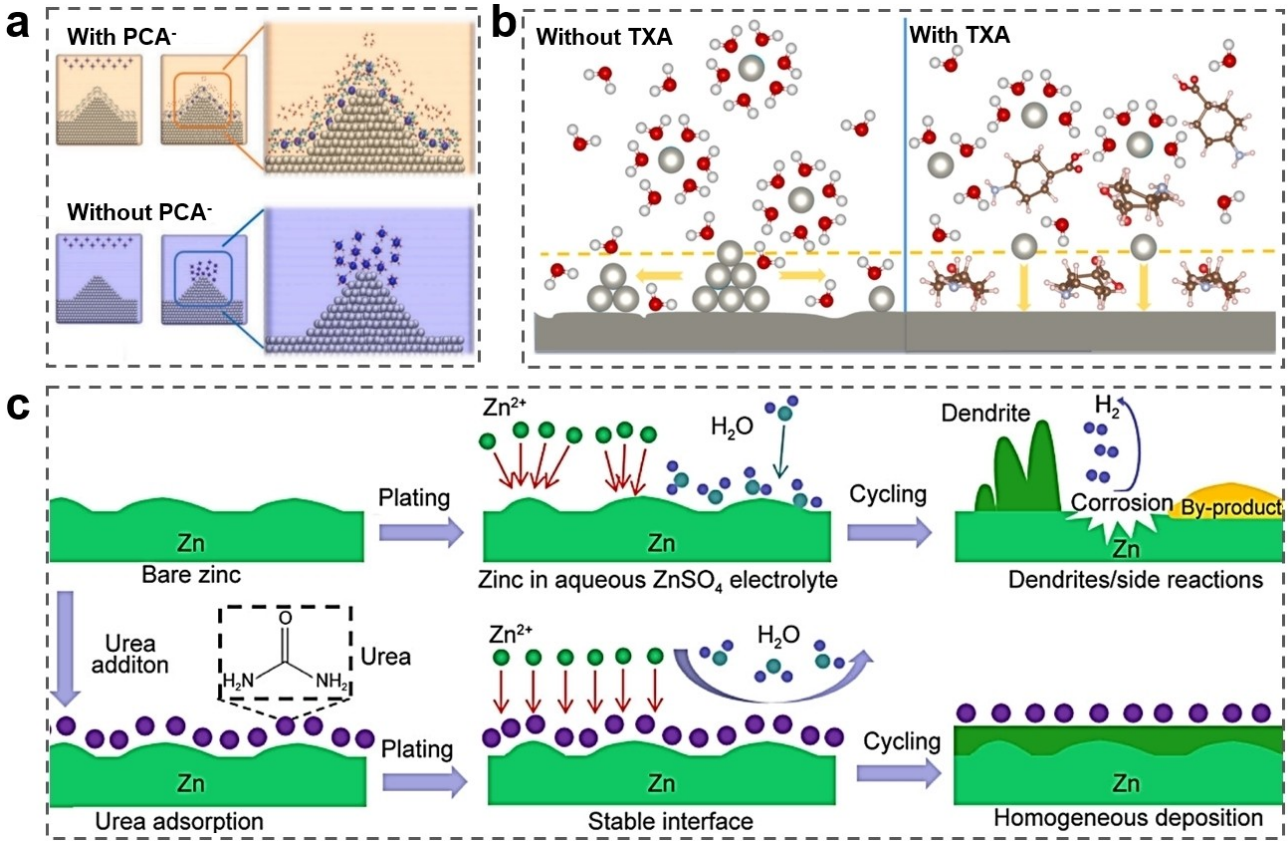

Figure 5. Reconstruction of Helmholtz plane on the interface of Zn–electrolyte. (a) Schematic illustration of the PCA^- layer on protrusion of Zn anode. Reproduced with permission from Ref. [60]. Copyright 2023 Elsevier. (b) Schematic illustration of the Zn–electrolyte interface with and without TXA. Reproduced with permission from Ref. [61]. Copyright 2023 Elsevier. (c) Schematic illustration of Zn deposition behavior in electrolytes with and without urea. Reproduced with permission from Ref. [62]. Copyright 2024 Springer Nature.

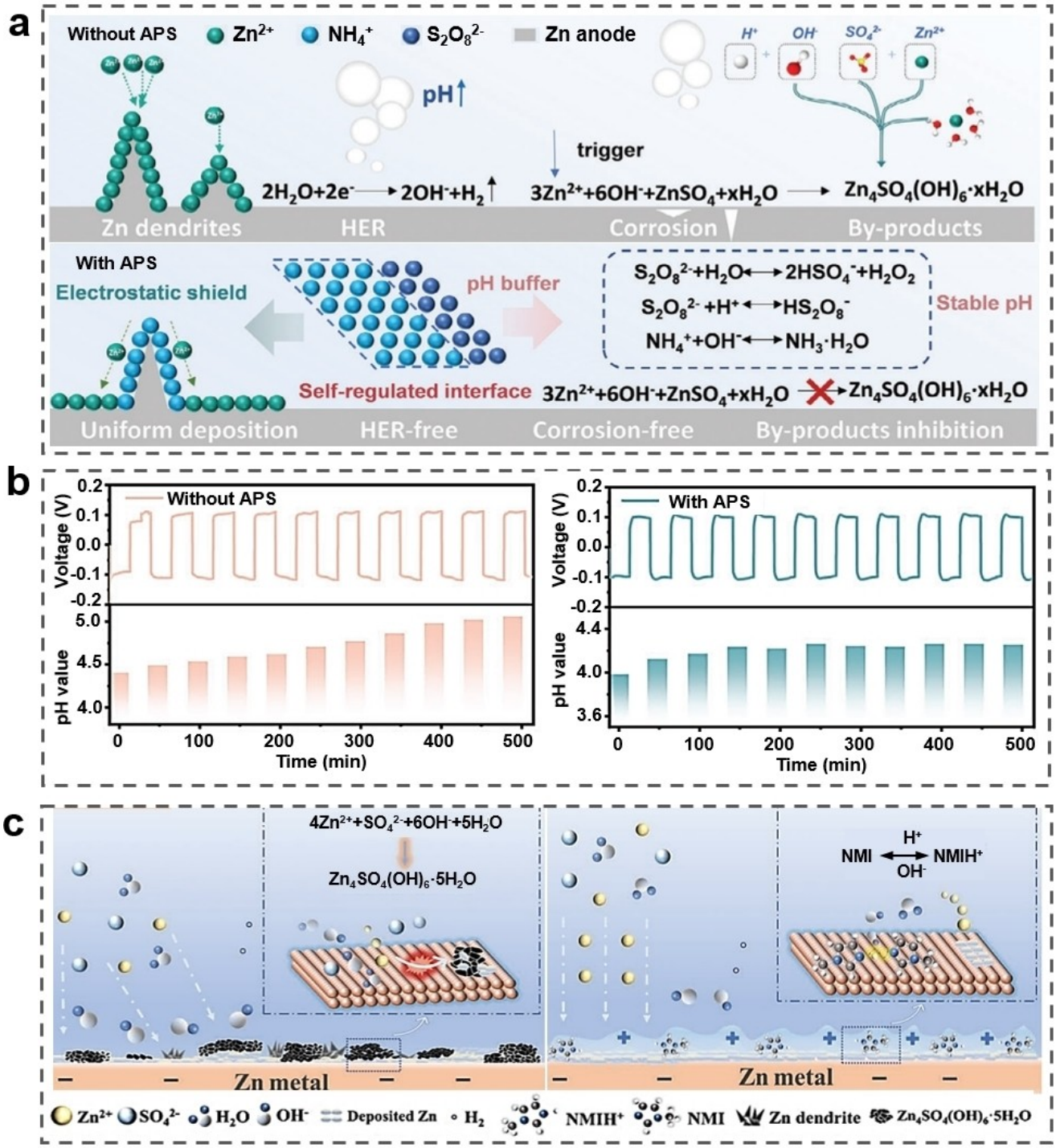

Figure 6. Stabilization of pH. (a) The schematic diagram of zinc plating processes in electrolytes with or without $(NH_4)_2S_2O_8$ (APS). Reproduced with permission from Ref. [54]. Copyright 2024 John Wiley and Sons. (b) In situ pH monitoring of different electrolytes at 5 mA cm^{-2}. Reproduced with permission from Ref. [54]. Copyright 2024 John Wiley and Sons. (c) Schematic illustrations of the improved reversibility of Zn anode in electrolyte with NMI. Reproduced with permission from Ref. [70]. Copyright 2023 John Wiley and Sons.

accumulation of by-products. As shown in Figure 6c, the NMI and $NMIH^+$ could adsorb on the Zn–electrolyte interface, forming a buffer layer. Upon hydrogen evolution, $NMIH^+$ released protons to neutralize by-products, transforming into NMI molecules. Subsequently, protons were transported to interfacial NMI via direct proton-hopping processes, thereby keeping a balance of $NMIH^+$ and NMI at the interface.[70] Han et al. employed ammonium acetate (NH_4OAc) as an additive to the $ZnSO_4$ electrolyte. They observed that NH_4^+ induced a dynamic electrostatic shielding layer around the Zn protuberances, ensuring the uniform Zn deposition, while OAc^- acted as an interfacial pH buffer, suppressing side reactions induced by

proton and the formation of by-products.[71] In addition, the ε-poly-l-lysine featuring numerous α-amino groups was also found to help maintain local pH stability.[72] The gelatin molecules with carboxyl groups could act as buffer components, adjusting the local pH of the Zn surface.[73] The mixed 2 M $ZnSO_4$ and 2 M $Zn(CF_3SO_3)_2$ electrolytes also exhibited strong pH buffering capabilities.[74]

3.3 Regulation of Kinetics

The transport of metal cations within the electrolyte is also a pivotal factor in determining the final morphologies of electroplated metals. Steep concentration gradients at the Zn–electrolyte interface can accelerate the growth of metal dendrites,[75] potentially extending into the bulk electrolyte where higher concentrations of cations are available.[76] This disparity between slow mass transfer and rapid electrochemical kinetics can lead to great concentration gradients on the surface of Zn electrode, resulting in uneven Zn deposition.

The hydrophilic groups, such as –OH, $–NH_2$, $–CONH_2$, $–SO_3H$, and –CONH–, have high adsorption affinity for polar solvent molecules. The strong interaction between functional groups and salt anions can enhance the cation transport properties, promoting the uniform Zn^{2+} distribution.[77] Qiu et al. utilized hyaluronic acid (HA) as a polymer additive in $ZnSO_4$ electrolyte. The abundant functional groups along the HA chains could facilitate the construction of effective tunnels for smooth Zn^{2+} transfer (Figure 7a). This enhancement was also evident in the improved Zn ion transference number, as shown in Figure 7b.[78] Similar results were also reported by other researchers. Shang et al. found that the alginate-based hydrogel electrolyte with ample carboxyl and hydroxyl groups could provide abundant bridge-linking positions for the multivalentcation-induced gelation (such as Ca^{2+}, Zn^{2+}, Na^{+}, and Fe^{3+}), easily transporting Zn^{2+} cations.[79] Yang et al. proposed that the steric hindrance of large-sized molecules (tributyl phosphate) could effectively slow down the charge transfer from the Zn anode to the solvated Zn^{2+}, thereby moderating the electrochemical reduction kinetics. Consequently, the preferential Zn deposition on the protrusion of anode was prevented, as illustrated in Figure 7c.[80] Other additives that can regulate the Zn^{2+} reduction kinetics were also reported. The sodium polystyrene sulfonate (PSS) compounds could encapsulate water shells around their chains, enhancing Zn^{2+} transport along the PSS chains and improving electrochemical performance.[81] Xylitol, with abundant polar polyhydroxy groups, could modulate the interaction of Zn^{2+} with H_2O and SO_4^{2-}, thereby reducing desolvation energy and enhancing Zn^{2+} migration.[82] Glycine (Gly), with carboxyl groups, could effectively capture Zn^{2+} through strong coordination, thereby alleviating disordered Zn^{2+} diffusion and regulating Zn^{2+} kinetics.[83]

Besides the regulation of Zn^{2+} transfer, the additive can also affect the Zn growth in the Zn plating process. Zn metal adopts a hexagonal close-packed structure, as depicted in Figure 8a. Among its crystal planes, the Zn(002) plane is considered to be the most stable.[84] Unlike the vertically aligned Zn(101) and Zn(110) planes, the Zn(002) plane accumulates parallelly.[85] According to the epitaxial mechanism, the smooth nature and even interfacial charge density of the Zn(002) plane favor uniform Zn deposition.[86] Additionally, this plane exhibits higher free energy of HER and stripping energy compared to Zn(110) plane, suggesting superior anti-corrosion properties.[87] Yang et al. suggested a spontaneous redox reaction between graphene oxide (GO) and the Zn anode, resulting in the reduced GO (rGO) layer on the Zn surface. This process promoted Zn nucleation in the $ZnSO_4$ electrolyte, transitioning from a 3D instantaneous to a 3D progressive mode. The Zn deposition demonstrated a Zn(002) orientation, thereby achieving desirable Zn plating/stripping kinetics.[88] Zhou et al. observed that sodium gluconate (SG) could shield Zn(100) and Zn(101) planes, leading to preferential adsorption of Zn^{2+} on the Zn(002) plane. It induced the planar growth of Zn as illustrated in Figure 8b.[89] Different from SG, the triethanolamine (TEOA) in 2 M $ZnSO_4$ electrolyte could preferentially adsorb on the Zn(002) plane. It retarded the growth of Zn(002) and enhanced its exposure, thereby facilitating dense and uniform Zn deposition.[90] Glycine exhibited higher electron transfer efficiency on Zn(002) compared with Zn(100) and Zn(101) plane. The adsorption of glycine on Zn(002) optimizes Zn^{2+} diffusion and nucleation behavior, consequently exposing the Zn(002) plane.[91] Other additives such as Tween-20 (TW20)[92] and 1-butyl-3-methylimidazolium cation ($BMIm^{+}$) were also reported to induce Zn(002)-oriented growth.[93]

While (002)-oriented Zn plating effectively suppresses Zn dendrite growth, the Zn(002) plane with higher chemical stability implies lower chemical activity. Thus, it necessitates higher polarization to facilitate Zn^{2+} transport.[94] Zhu et al. claimed that the Zn(100) plane with the highest adsorption energy with Zn atoms had the lowest Zn stripping energy. By introducing disodium lauryl phosphate (DLP) to the $ZnSO_4$ electrolyte, vertically oriented Zn plating could be achieved, resulting in the preferential growth of the Zn(100) plane. As shown in Figure 8c, the selective adsorption of phosphoric acid groups on the surface of the Zn(002) plane could promote the vertically oriented Zn plating, exhibiting Zn(100) plane.[95] Additionally, Hu et al. suggested that serine could adsorb on the Zn(100) plane, thereby restricting Zn(100)-orientation growth. The preferred (100) texture could lead to a smooth and dendrite-free surface.[96] It can be concluded that the oriented growth of Zn induced by additives can result in uniform Zn deposition.

4. Summary and Outlooks

In this study, we elucidate recent advancements in electrolyte composition and additive usage in aqueous ZIBs aimed at stabilizing the Zinc anode, as summarized in Table 1. The presence of water molecules with dipoles is prone to accumulate in the Helmholtz layer. The water molecules within the EDL can serve as reactants for the HER. The water-in-salt electrolyte, eutectic electrolytes, and weakly solvating electrolytes need

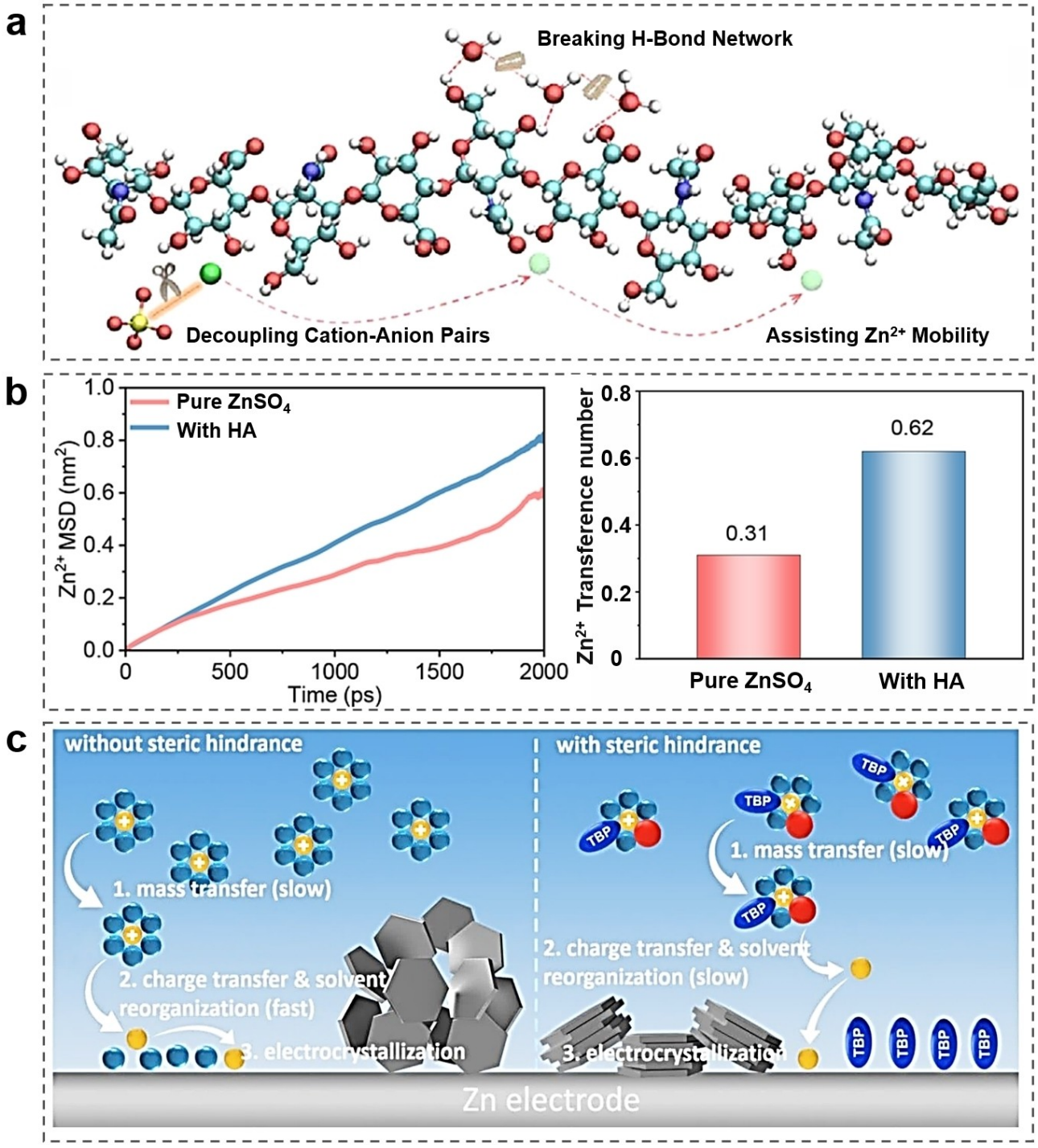

Figure 7. Regulation of Zn^{2+} transfer. (a) Scheme illustrating the chain-type structure and the electrostatic potential mapping of the HA molecules. Reproduced with permission from Ref. [78]. Copyright 2022 American Chemical Society. (b) MSD as a function of time under different electrolytes and the calculated Zn^{2+} transference number of different electrolyte. Reproduced with permission from Ref. [78]. Copyright 2022 American Chemical Society. (c) Illustration of suppressed Zn dendrite by regulating the electrochemical reduction process. Reproduced with permission from Ref. [80]. Copyright 2024 Royal Society of Chemistry.

high concentration salt or solvent, which may counteract the advantages of ZIB on safety and price. $ZnSO_4$-based electrolytes, known for their cost-effectiveness and high ionic conductivity, are extensively employed in ZIBs. Introducing additives offers a feasible and economically viable solution to challenges encountered in ZIBs, including the Zn dendrite and side reactions. Chemicals with highly polar groups such as carboxyl, amino, and hydroxyl groups, can interact with electrolyte components, effectively modulating the Zn^{2+} reduction process and resulting in uniform Zn deposition. Biomass materials, characterized by

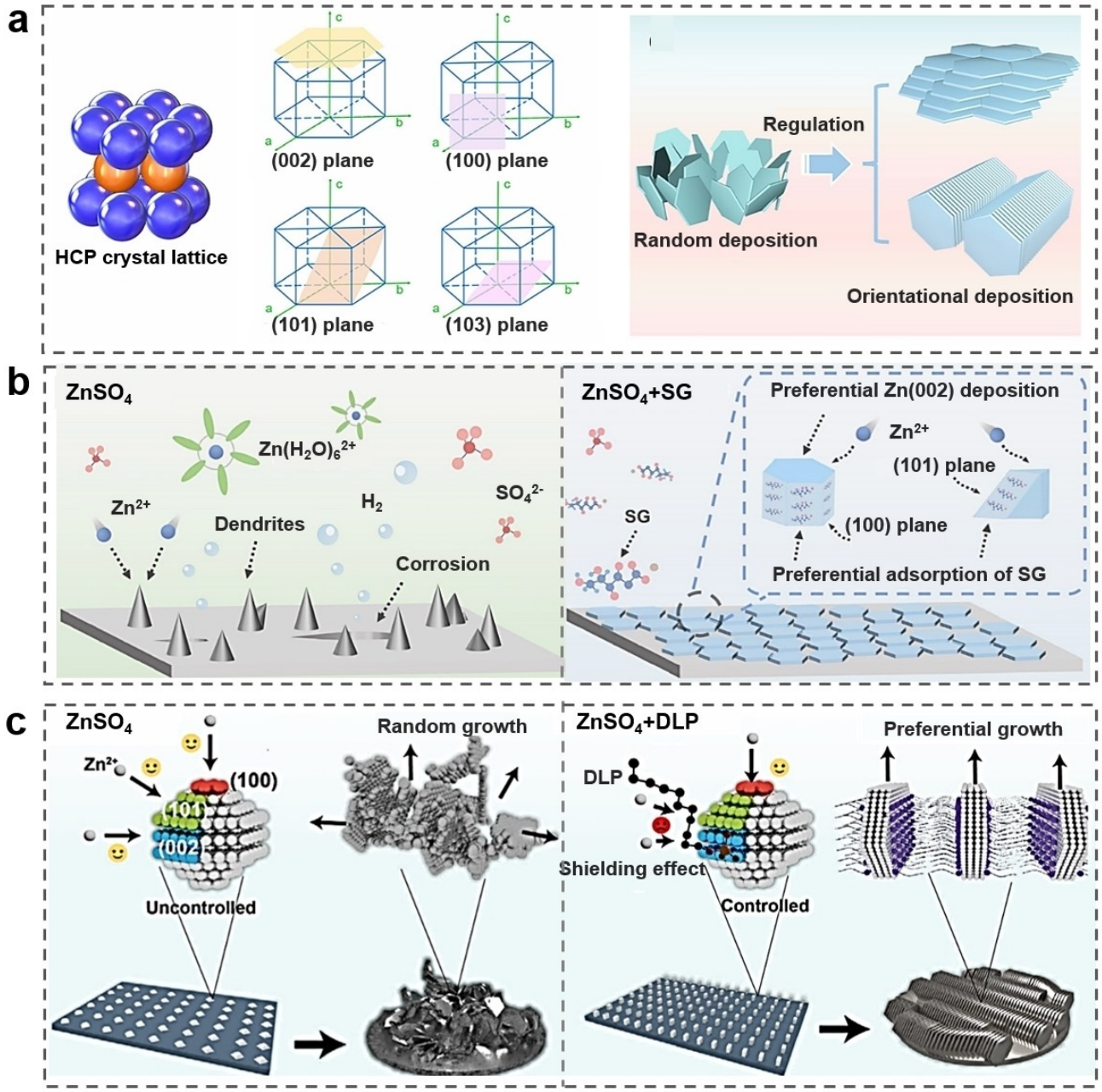

Figure 8. The orientational Zn growth. (a) Schematic illustration of a HCP crystal and specific lattice planes of Zn and the Zn deposition behavior. Reproduced with permission from Ref. [94]. Copyright 2022 Royal Society of Chemistry. (b) Schematic illustrations of Zn deposition with and without SG. Reproduced with permission from Ref. [89]. Copyright 2024 Royal Society of Chemistry. (c) Schematic illustration of vertically oriented Zn plating modulated by selective shielding of the (002) plane. Reproduced with permission from Ref. [95]. Copyright 2023 John Wiley and Sons.

eco-friendliness, diverse architectures, enriched surface chemistry, and low cost (such as Glucose, Carboxymethylcellulose sodium, and Gum arabic in Table 1, the cost is obtained from Shanghai Aladdin Biochemical Technology Co., Ltd.), show significant potential in this regard. Exploring the utilization of biomass materials in ZIBs presents an avenue for enhancing performance while ensuring environmental sustainability. However, due to the lack of harmonized test standards and reagent standards, it is not possible to accurately assess the economics of each additive strategy to enhance the stability of zinc anode. Though numerous achievements have been attained in electrolytes to stabilize the Zn anode, herein, we put forward some suggestions to promote the future development of electrolytes from the following viewpoints:

(1) The underlying principles governing the effects of various additive groups on stabilizing the Zn anode should be illuminated. The standardized test methods should be built for future statistical analysis and prediction by machine learning.
(2) More in situ characterization methods should be applied to monitor the real reaction process, such as holographic analysis of concentration gradient, in situ confocal imaging

Table 1. Summary of the Zn||Zn symmetric cell performances in different electrolytes.

Electrolyte components	Addition and its cost	Current density ($mA\,cm^{-2}$)	Areal capacity ($mAh\,cm^{-2}$)	Lifespan (h)	Refs.
2 M $Zn(OTF)_2$ – (1 TMS – 1 H_2O)	Tetramethylene sulfone, 17 $\$\,kg^{-1}$	1	1	1800	[35]
2 M $Zn(BF_4)_2$ – (1 ace −1 H_2O)	Acetamide (Ace), 20 $\$\,kg^{-1}$	1	0.5	1300	[36]
1.6 M $ZnSO_4$ – 20% ETH	Ethanol, 13 $\$\,L^{-1}$	1	1	2000	[39]
1 M $Zn(OTF)_2$ – 50 v/v% acetone	Acetone, 48 $\$\,L^{-1}$	1	1	800	[40]
1.6 M $ZnCl_2$ – 20 v/v% DMSO	Dimethyl sulfoxide (DMSO), 51 $\$\,L^{-1}$	0.5	0.5	1000	[41]
1 M $ZnSO_4$ – 10 mM glucose	Glucose, 21 $\$\,kg^{-1}$	1	1	2000	[43]
2 M $ZnSO_4$ – 2% GBL	Gamma butyrolactone (GBL), 24 $\$\,kg^{-1}$	10	10	1170	[44]
2 M $ZnSO_4$ – 1.5 wt.% DTPA-Na	Penta-sodium diethylene-triaminepentaacetic acid salt (DTPA–Na), 59 $\$\,kg^{-1}$	2	1	800	[45b]
2 M $ZnSO_4$ – 1% GA	Gum arabic (GA), 33 $\$\,kg^{-1}$	2.5	0.5	3600	[45c]
2 M $ZnSO_4$ – 1 mg/mL CMC	Carboxymethylcellulose sodium (CMC), 28 $\$\,kg^{-1}$	1	1	3125	[54]
1 M $ZnSO_4$ – 0.5 wt.% SF	Silk fibroin (SF), 188117 $\$\,kg^{-1}$	1	1	1600	[55]
2 M ZnSO4 – 1 wt.% FEP	Tris(2,2,2-trifluoroethyl) Phosphate (FEP), 387 $\$\,kg^{-1}$	10	10	1800	[56]
2 M ZnSO4 – 1 wt.% DX	Dioxane (DX), 38 $\$\,L^{-1}$	2	2	1300	[57]
2 M $ZnSO_4$ – 200 mM [EMIM]OTF	1-ethyl-3-methylimidazole trifluoromethanesulfonate ([EMIM]OTF, 1203 $\$\,kg^{-1}$	5	5	900	[59a]
2 M $ZnSO_4$ – 2 mM KTPP	Penta-potassium triphosphate (KTPP), 22 $\$\,kg^{-1}$	2	2	2500	[59b]
1.8 M $ZnSO_4$ – 0.2 M PCA-Zn	Zinc pyrrolidone carboxylate (PCA–Zn), 166 $\$\,kg^{-1}$	5	5	650	[60]
2 M $ZnSO_4$ – 50 mM TXA	Trifunctional tranexamic acid (TAX), 174 $\$\,kg^{-1}$	5	5	700	[61]
1 M $ZnSO_4$ – 20 mM urea	Urea, 14 $\$\,kg^{-1}$	5	5	2100	[62]
2 M $ZnSO_4$ – 0.3 M Gln	Glutamine (Gln), 44 $\$\,kg^{-1}$	3	3	700	[64]
3 M $ZnSO_4$ – 5 mM HMTA	Hexamethylenetetramine (HMTA), 61 $\$\,kg^{-1}$	5	1	4000	[65]
2 M $ZnSO_4$ – 0.1 M APS	$(NH_4)_2S_2O_8$ (APS), 26 $\$\,kg^{-1}$	5	5	1200	[69]
2 M $ZnSO_4$ – 0.2 M NMI	N-methylimidazole (NMI), 57 $\$\,L^{-1}$	1	1	2600	[70]
1 M $ZnSO_4$ – 0.8 mg/mL HA	Hyaluronic acid (HA), 797253$ kg^{-1}	5	5	800	[78]
1 M $Zn(TFSI)_2$ – (0.5 EMC – 0.5 TBP – 1 H_2O)	Tributyl phosphate (TBP), 28 $\$\,L^{-1}$	2	1	2100	[80]
1 M $Zn(OTF)_2$ – 2%PSS	Sodium polystyrene sulfonate (PSS), 1331 $\$\,kg^{-1}$	1	1	3000	[81]
2 M $ZnSO_4$ – 100 mM xylitol	Xylitol, 61 $\$\,kg^{-1}$	5	1	1000	[82]
2 M $ZnSO_4$ – 20 mM SG	Sodium gluconate (SG), 32 $\$\,kg^{-1}$	5	2.5	900	[89]
2 M $ZnSO_4$ – 0.5 M TEOA	Triethanolamine (TEOA), 76 $\$\,L^{-1}$	2	1	2200	[90]
2 M $ZnSO_4$ – 20 mg/mL Glycine	Glycine, 18 $\$\,kg^{-1}$	1	1	3100	[91]
2 M $ZnSO_4$ – 2.0% TW20	Tween-20 (TW20), 40 $\$\,L^{-1}$	5	5	500	[92]
2 M $ZnSO_4$ – 0.02 M $BMIm^+$	1-butyl-3-methylimidazolium trifluoromethanesulfonate (BMImOTf), 832 $\$\,kg^{-1}$	5	5	1400	[93]
2 M $ZnSO_4$ – 0.01 M DLP	Disodium lauryl phosphate (DLP), 829 $\$\,kg^{-1}$	10	10	700	[94]
3 M $ZnSO_4$ – 10 wt.% serine	Serine, 100 $\$\,kg^{-1}$	5	5	800	[96]
2 M $ZnSO_4$ – 0.01 M TA	Tannic acid, 142 $\$\,kg^{-1}$	10	5	500	[97]

of interface uniformity and growth dynamics, and in situ DEMS/EQCM analysis of side reactions.

(3) The current research focuses on the materials, but the electrolyte is generally added excessively. To reflect the real effect of electrolyte, it should be evaluated in devices with limited N/P ratio (ratio of negative to positive electrode capacity), and E/C ratio (ratio of electrolyte addition to positive electrode capacity).

Acknowledgements

This work was financially supported by the National Natural Science Foundation of China (No. 22279023, 22075115, and 22309031), the Natural Science Foundation of the Jiangsu Higher Education Institutions of China (No. 21KJA150005, 21KJB430044 and 23KJB480009), the Xuzhou Science and Technology Project (No. KC22301 and KC23033), and Shanghai

Science and Technology Innovation Action Plan Morning Star Project (Sail Special) (No. 23YF1401800).

Conflict of Interests

The authors declare no conflict of interest.

Keywords: Zn metal aqueous batteries · Electrolyte · Additive · Mechanism · Long lifespan

[1] W. Zhang, Q. Dong, J. Wang, X. Han, W. Hu, *Small Methods* **2023**, *7*, 2300324.
[2] J. Yang, R. Zhao, Y. Wang, Z. Hu, Y. Wang, A. Zhang, C. Wu, Y. Bai, *Adv. Funct. Mater.* **2023**, *33*, 2213510.
[3] C. Nie, G. Wang, D. Wang, M. Wang, X. Gao, Z. Bai, N. Wang, J. Yang, Z. Xing, S. Dou, *Adv. Energy Mater.* **2023**, *13*, 2300606.
[4] a) Y. Shen, H. Lv, L. Chen, *Mater. Chem. Front.* **2023**, *7*, 2376–2404; b) J. Zheng, Z. Huang, F. Ming, Y. Zeng, B. Wei, Q. Jiang, Z. Qi, Z. Wang, H. Liang, *Small* **2022**, *18*, e2200006.
[5] a) Y. Zong, H. He, Y. Wang, M. Wu, X. Ren, Z. Bai, N. Wang, X. Ning, S. X. Dou, *Adv. Energy Mater.* **2023**, *7*, 2373–2404; b) W. Wang, C. Li, S. Liu, J. Zhang, D. Zhang, J. Du, Q. Zhang, Y. Yao, *Adv. Energy Mater.* **2023**, *13*, 2300250.
[6] a) Y. Xu, X. Zhou, Z. Chen, Y. Hou, Y. You, J. Lu, *Mater. Today* **2023**, *66*, 339–347; b) J. Zhao, H. Lu, J. Peng, X. Li, J. Zhang, B. Xu, *Energy Storage Mater.* **2023**, *60*, 102846.
[7] a) X. Zhang, J. Chen, H. Cao, X. Huang, Y. Liu, Y. Chen, Y. Huo, D. Lin, Q. Zheng, K. h Lam, *Small* **2023**, *19*, 2303906; b) S. Zhang, M. Ye, Y. Zhang, Y. Tang, X. Liu, C. C. Li, *Adv. Funct. Mater.* **2023**, *33*, 2208230.
[8] a) A. Yu, W. Zhang, N. Joshi, Y. Yang, *Energy Storage Mater.* **2024**, *64*, 103075; b) B. Wang, H. Xu, J. Hao, J. Du, C. Wu, Z. Ma, W. Qin, *Batteries* **2023**, *9*, 73.
[9] a) R. Zhang, Y. Feng, Y. Ni, B. Zhong, M. Peng, T. Sun, S. Chen, H. Wang, Z. Tao, K. Zhang, *Angew. Chem. Int. Ed.* **2023**, *62*, e202304503; b) C. You, R. Wu, X. Yuan, J. Ye, L. Liu, L. Fu, P. Han, Y. Wu, *Energy Environ. Sci.* **2023**, *16*, 5096–5107; c) Q. Wen, H. Fu, R. D. Cui, H. Z. Chen, R. H. Ji, L. B. Tang, C. Yan, J. Mao, K. H. Dai, X. H. Zhang, J. C. Zheng, *J. Energy Chem.* **2023**, *83*, 287–303.
[10] a) Y. Zhang, Y. Liu, Z. Liu, X. Wu, Y. Wen, H. Chen, X. Ni, G. Liu, J. Huang, S. Peng, *J. Energy Chem.* **2022**, *64*, 23–32; b) Y. Zhang, A. Chen, J. Sun, *J. Energy Chem.* **2021**, *54*, 655–667; c) Y. Li, J. Zhao, Q. Hu, T. Hao, H. Cao, X. Huang, Y. Liu, Y. Zhang, D. Lin, Y. Tang, Y. Cai, *Mater. Today* **2022**, *29*, 101095.
[11] a) Q. Yang, Q. Li, Z. Liu, D. Wang, Y. Guo, X. Li, Y. Tang, H. Li, B. Dong, C. Zhi, *Adv. Mater.* **2020**, *32*, e2001854; b) G. Yoo, Y. G. Lee, B. Im, D. G. Kim, Y. R. Jo, G. H. An, *Energy Storage Mater.* **2023**, *61*, 102845.
[12] C. Li, X. Xie, S. Liang, J. Zhou, *Energy Environ.* **2020**, *3*, 146–159.
[13] a) D. Xie, Z. W. Wang, Z. Y. Gu, W. Y. Diao, F. Y. Tao, C. Liu, H. Z. Sun, X. L. Wu, J. W. Wang, J. P. Zhang, *Adv. Funct. Mater.* **2022**, *32*, 2204066; b) Z. Zhao, J. Zhao, Z. Hu, J. Li, J. Li, Y. Zhang, C. Wang, G. Cui, *Energy Environ. Sci.* **2019**, *12*, 1938–1949; c) T. Wang, P. Wang, L. Pan, Z. He, L. Dai, L. Wang, S. Liu, S. C. Jun, B. Lu, S. Liang, J. Zhou, *Adv. Energy Mater.* **2022**, *13*, 2203523.
[14] a) Y. Liu, S. Liu, X. Xie, Z. Li, P. Wang, B. Lu, S. Liang, Y. Tang, J. Zhou, *InfoMat* **2023**, *5*, e12374; b) Y. Zhang, G. Yang, M. L. Lehmann, C. Wu, L. Zhao, T. Saito, Y. Liang, J. Nanda, Y. Yao, *Nano Lett.* **2021**, *21*, 10446–10452.
[15] a) W. Guo, T. Hua, C. Qiao, Y. Zou, Y. Wang, J. Sun, *Energy Storage Mater.* **2024**, *66*, 103244; b) J. Li, Z. Guo, J. Wu, Z. Zheng, Z. Yu, F. She, L. Lai, H. Li, Y. Chen, L. Wei, *Adv. Energy Mater.* **2023**, *13*, 2301743; c) Z. Khan, D. Kumar, X. Crispin, *Adv. Mater.* **2023**, *35*, 2300369.
[16] S. Bai, Z. Huang, G. Liang, R. Yang, D. Liu, W. Wen, X. Jin, C. Zhi, X. Wang, *Adv. Sci.* **2023**, *11*, 2304549.
[17] a) N. Zhang, F. Cheng, Y. Liu, Q. Zhao, K. Lei, C. Chen, X. Liu, J. Chen, *J. Am. Chem. Soc.* **2016**, *138*, 12894–12901; b) H. Wang, X. Liu, J. Zhong, L. Du, S. Yun, X. Zhang, Y. Gao, L. Kang, *Small* **2024**, *20*, 2306947.
[18] L. Sun, Z. Song, C. Deng, Q. Wang, F. Mo, H. Hu, G. Liang, *Batteries* **2023**, *9*, 386.
[19] Z. Hou, Z. Lu, Q. Chen, B. Zhang, *Energy Storage Mater.* **2021**, *42*, 517–525.
[20] Q. Li, A. Chen, D. Wang, Z. Pei, C. Zhi, *Joule* **2022**, *6*, 273–279.
[21] L. Kang, M. Cui, F. Jiang, Y. Gao, H. Luo, J. Liu, W. Liang, C. Zhi, *Adv. Energy Mater.* **2018**, *8*, 1801090.
[22] a) T. Mageto, S. D. Bhoyate, K. Mensah-Darkwa, A. Kumar, R. K. Gupta, *J. Energy Storage* **2023**, *70*, 108081; b) J. R. Loh, J. Xue, W. S. V. Lee, *Small Methods* **2023**, *7*, 2300101.
[23] X. Liu, H. Euchner, M. Zarrabeitia, X. Gao, G. A. Elia, A. Groß, S. Passerini, *ACS Energy Lett.* **2020**, *5*, 2979–2986.
[24] L. Zhang, I. A. Rodríguez-Pérez, H. Jiang, C. Zhang, D. P. Leonard, Q. Guo, W. Wang, S. Han, L. Wang, X. Ji, *Adv. Funct. Mater.* **2019**, *29*, 1902653.
[25] M. Li, Z. Li, X. Wang, J. Meng, X. Liu, B. Wu, C. Han, L. Mai, *Energy Environ. Sci.* **2021**, *14*, 3796–3839.
[26] J. Zhang, J. Sun, D. Yang, S. Ha, T. Ma, H. Liu, X. Shi, D. Guo, Y. Wang, Y. Wei, *Nano Lett.* **2024**, *24*, 688–695.
[27] D. Wang, Q. Li, Y. Zhao, H. Hong, H. Li, Z. Huang, G. Liang, Q. Yang, C. Zhi, *Adv. Energy Mater.* **2022**, *12*, 2102707.
[28] D. Xiao, L. Zhang, Z. Li, H. Dou, X. Zhang, *Energy Storage Mater.* **2022**, *44*, 10–28.
[29] F. Wang, O. Borodin, T. Gao, X. Fan, W. Sun, F. Han, A. Faraone, J. A. Dura, K. Xu, C. Wang, *Nat. Mater.* **2018**, *17*, 543–549.
[30] C. Zhang, J. Holoubek, X. Wu, A. Daniyar, L. Zhu, C. Chen, D. P. Leonard, I. A. Rodríguez-Pérez, J. X. Jiang, C. Fang, X. Ji, *Chem. Commun.* **2018**, *54*, 14097–14099.
[31] A. Clarisza, H. K. Bezabh, S. K. Jiang, C. J. Huang, B. W. Olbasa, S. H. Wu, W. N. Su, B. J. Hwang, *ACS Appl. Mater. Interfaces* **2022**, *14*, 36644–36655.
[32] J. Han, A. Mariani, A. Varzi, S. Passerini, *J. Power Sources* **2021**, *485*, 229329.
[33] Y. Zhu, J. Yin, X. Zheng, A.-H. Emwas, Y. Lei, O. F. Mohammed, Y. Cui, H. N. Alshareef, *Energy Environ. Sci.* **2021**, *14*, 4463–4473.
[34] Z. Zhang, Z. He, N. Wang, F. Wang, C. Du, J. Ruan, Q. Li, D. Sun, F. Fang, F. Wang, *Adv. Funct. Mater.* **2023**, *33*, 2214648.
[35] Y. Zhong, X. Xie, Z. Zeng, B. Lu, G. Chen, J. Zhou, *Angew. Chem. Int. Ed.* **2023**, *62*, e202310577.
[36] S. Wang, S. Chen, Y. Ying, G. Li, H. Wang, K. K. K. Cheung, Q. Meng, H. Huang, L. Ma, J. A. Zapien, *Angew. Chem. Int. Ed.* **2024**, *63*, e202316841.
[37] W. Deng, Z. Deng, Y. Chen, R. Feng, X. Wang, *Angew. Chem. Int. Ed.* **2024**, *63*, e202316499.
[38] Y. Yang, G. Qu, H. Wei, Z. Wei, C. Liu, Y. Lin, X. Li, C. Han, C. Zhi, H. Li, *Adv. Energy Mater.* **2023**, *13*, 2203729.
[39] K. Bao, M. Wang, Y. Zheng, P. Wang, L. Yang, Y. Jin, H. Wu, B. Sun, *Nano Energy* **2024**, *120*, 109089.
[40] X. Cao, W. Xu, D. Zheng, F. Wang, Y. Wang, X. Shi, X. Lu, *Angew. Chem. Int. Ed.* **2024**, *63*, e202317302.
[41] L. Cao, D. Li, E. Hu, J. Xu, T. Deng, L. Ma, Y. Wang, X. Q. Yang, C. Wang, *J. Am. Chem. Soc.* **2020**, *142*, 21404–21409.
[42] Q. Shen, Y. Wang, G. Han, X. Li, T. Yuan, H. Sun, Y. Gong, T. Chen, *Batteries* **2023**, *9*, 284.
[43] P. Sun, L. Ma, W. Zhou, M. Qiu, Z. Wang, D. Chao, W. Mai, *Angew. Chem. Int. Ed.* **2021**, *60*, 18247–18255.
[44] H. Huang, D. Xie, J. Zhao, P. Rao, W. M. Choi, K. Davey, J. Mao, *Adv. Energy Mater.* **2022**, *12*, 2202419.
[45] a) Y. Xiong, Q. Li, K. Luo, L. Zhong, G. Li, S. Zhong, D. Yan, *J. Energy Storage* **2023**, *68*, 107655; b) Y. Xia, R. Tong, J. Zhang, M. Xu, G. Shao, H. Wang, Y. Dong, C. A. Wang, *Nano-Micro Lett.* **2024**, *16*, 82; c) H. Zheng, Y. Huang, J. Xiao, W. Zeng, X. Li, X. Li, M. Wang, Y. Lin, *Chem. Eng. J.* **2023**, *468*, 143834.
[46] B. Qiu, L. Xie, G. Zhang, K. Cheng, Z. Lin, W. Liu, C. He, P. Zhang, H. Mi, *Chem. Eng. J.* **2022**, *449*, 137843.
[47] C. Xie, S. Liu, H. Wu, Q. Zhang, C. Hu, Z. Yang, H. Li, Y. Tang, H. Wang, *Sci. Bull.* **2023**, *68*, 1531–1539.
[48] K. Qiu, G. Ma, Y. Wang, M. Liu, M. Zhang, X. Li, X. Qu, W. Yuan, X. Nie, N. Zhang, *Adv. Funct. Mater.* **2024**, *34*, 2313358.
[49] H. Yang, Y. Qiao, Z. Chang, H. Deng, X. Zhu, R. Zhu, Z. Xiong, P. He, H. Zhou, *Adv. Mater.* **2021**, *33*, 2102415.
[50] W. Shang, Q. Li, F. Jiang, B. Huang, J. Song, S. Yun, X. Liu, H. Kimura, J. Liu, L. Kang, *Nano-Micro Lett.* **2022**, *14*, 82.
[51] T. Yan, M. Tao, J. Liang, G. Zheng, B. Wu, L. Du, Z. Cui, H. Song, *Energy Storage Mater.* **2024**, *65*, 103190.
[52] a) H. Yan, S. Li, J. Zhong, B. Li, *Nano-Micro Lett.* **2023**, *16*, 15; b) R. Jayakumar, D. M. Harrison, J. Xu, A. V. Suresh Babu, C. Luo, L. Ma, *J. Mater. Chem. A* **2023**, *11*, 8470–8496.
[53] X. Xu, X. Zhu, S. Li, Y. Xu, L. Sun, L. Shi, M. Song, *J. Electron. Mater.* **2023**, *53*, 288–297.

[54] Y. Song, W. Lu, H. Yang, C. Wu, W. Wei, G. Kuang, Y. Chen, L. Chen, X. Ouyang, *Nano Energy* **2024**, *120*, 109094.
[55] J. Xu, W. Lv, W. Yang, Y. Jin, Q. Jin, B. Sun, Z. Zhang, T. Wang, L. Zheng, X. Shi, B. Sun, G. Wang, *ACS Nano* **2022**, *16*, 11392–11404.
[56] L. Wang, P. P. Wang, H. Q. Zhou, Z. B. Wang, C. Y. Xu, *Nano Energy* **2024**, *119*, 109076.
[57] G. Zhang, J. Zhu, K. Wang, Q. Li, W. Fu, X. X. Liu, X. Sun, *Chem. Commun.* **2024**, *60*, 1317–1320.
[58] W. Xin, L. Miao, L. Zhang, H. Peng, Z. Yan, Z. Zhu, *ACS Materials Lett.* **2021**, *3*, 1819–1825.
[59] a) J. Weng, W. Zhu, K. Yu, J. Luo, M. Chen, L. Li, Y. Zhuang, K. Xia, Z. Lu, Y. Hu, C. Yang, M. Wu, Z. Zou, *Advanced Functional Materials* **2024**, *34*, 2314347; b) Y. Yu, P. Zhang, W. Wang, J. Liu, *Small Methods* **2023**, *7*, 2300546.
[60] S. jiao, J. Fu, Q. Yin, H. Yao, H. Hu, *Energy Storage Mater.* **2023**, *59*, 102774.
[61] J. Yin, H. Liu, P. Li, X. Feng, M. Wang, C. Huang, M. Li, Y. Su, B. Xiao, Y. Cheng, X. Xu, *Energy Storage Mater.* **2023**, *59*, 102800.
[62] B. R. Xu, Q. A. Li, Y. Liu, G. B. Wang, Z. H. Zhang, F. Z. Ren, *Rare Met.* **2024**, *43*, 1599–1609.
[63] X. Xu, M. Song, M. Li, Y. Xu, L. Sun, L. Shi, Y. Su, C. Lai, C. Wang, *Chem. Eng. J.* **2023**, *454*, 140364.
[64] J. Yin, M. Li, X. Feng, T. Cui, J. Chen, F. Li, M. Wang, Y. Cheng, S. Ding, X. Xu, J. Wang, *J. Mater. Chem. A* **2024**, *12*, 1543–1550.
[65] H. Yu, D. Chen, Q. Li, C. Yan, Z. Jiang, L. Zhou, W. Wei, J. Ma, X. Ji, Y. Chen, L. Chen, *Adv. Energy Mater.* **2023**, *13*, 2300550.
[66] H. Wang, H. Du, R. Zhao, Z. Zhu, L. Qie, J. Fu, Y. Huang, *Adv. Funct. Mater.* **2023**, *33*, 2213803.
[67] C. Lin, L. He, P. Xiong, H. Lin, W. Lai, X. Yang, F. Xiao, X.-L. Sun, Q. Qian, S. Liu, Q. Chen, S. Kaskel, L. Zeng, *ACS Nano* **2023**, *17*, 23181–23193.
[68] J. Cao, D. Zhang, X. Zhang, Z. Zeng, J. Qin, Y. Huang, *Energy Environ. Sci.* **2022**, *15*, 499–528.
[69] H. Li, L. Yang, S. Zhou, J. Li, Y. Chen, X. Meng, D. Xu, C. Han, H. Duan, A. Pan, *Advanced Functional Materials* **2024**, *34*, 2313859.
[70] M. Zhang, H. Hua, P. Dai, Z. He, L. Han, P. Tang, J. Yang, P. Lin, Y. Zhang, D. Zhan, J. Chen, Y. Qiao, C. C. Li, J. Zhao, Y. Yang, *Advanced Materials* **2023**, *35*, 2208630.
[71] D. Han, Z. Wang, H. Lu, H. Li, C. Cui, Z. Zhang, R. Sun, C. Geng, Q. Liang, X. Guo, Y. Mo, X. Zhi, F. Kang, Z. Weng, Q. H. Yang, *Adv. Energy Mater.* **2022**, *12*, 2102982.
[72] Y. Guo, Z. Li, B. Niu, H. Chen, Y. Qiao, Y. Min, X. Wang, *Small* **2024**, *20*, 2310341.
[73] Y. Wu, N. Wang, H. Liu, R. Cui, J. Gu, R. Sun, Y. Zhu, L. Gou, X. Fan, D. Li, D. Wang, *J. Colloid Interface Sci.* **2023**, *629*, 916–925.
[74] S. Jin, F. Duan, X. Wu, J. Li, X. Dan, X. Yin, K. Zhao, Y. Wei, Y. Sui, F. Du, Y. Wang, *Small* **2022**, *18*, e2205462.
[75] J. Liu, Z. Bao, Y. Cui, E. J. Dufek, J. B. Goodenough, P. Khalifah, Q. Li, B. Y. Liaw, P. Liu, A. Manthiram, Y. S. Meng, V. R. Subramanian, M. F. Toney, V. V. Viswanathan, M. S. Whittingham, J. Xiao, W. Xu, J. Yang, X. Q. Yang, J. G. Zhang, *Nat. Energy* **2019**, *4*, 180–186.
[76] J. Xiao, *Science* **2019**, *366*, 426–427.
[77] Y. Zhang, M. Xu, X. Jia, F. Liu, J. Yao, R. Hu, X. Jiang, P. Yu, H. Yang, *Molecules* **2023**, *28*, 2436.
[78] M. Qiu, P. Sun, G. Cui, W. Mai, *ACS Appl. Mater. Interfaces* **2022**, *14*, 40951–40958.
[79] W. Shang, J. Zhu, Y. Liu, L. Kang, S. Liu, B. Huang, J. Song, X. Li, F. Jiang, W. Du, Y. Gao, H. Luo, *ACS Appl. Mater. Interfaces* **2021**, *13*, 24756–24764.
[80] S. Yang, A. Chen, Z. Tang, Z. Wu, P. Li, Y. Wang, X. Wang, J. Xu, S. Bai, C. Zhi, *Energy Environ. Sci.* **2024**, *17*, 1095–1106.
[81] Y. Wu, T. Zhang, L. Chen, Z. Zhu, L. Cheng, S. Gu, Z. Li, Z. Tong, H. Li, Y. Li, Z. Lu, W. Zhang, C. S. Lee, *Adv. Energy Mater.* **2023**, *13*, 2300719.
[82] H. Wang, W. Ye, B. Yin, K. Wang, M. S. Riaz, B. B. Xie, Y. Zhong, Y. Hu, *Angewandte Chemie International Edition* **2023**, *62*, e202218872.
[83] Z. Luo, Y. Xia, S. Chen, X. Wu, R. Zeng, X. Zhang, H. Pan, M. Yan, T. Shi, K. Tao, B. B. Xu, Y. Jiang, *Nano-Micro Lett.* **2023**, *15*, 205.
[84] W. Yuan, X. Nie, G. Ma, M. Liu, Y. Wang, S. Shen, N. Zhang, *Angew. Chem. Int. Ed.* **2023**, *62*, e202218386.
[85] Z. Huang, Z. Li, Y. Wang, J. Cong, X. Wu, X. Song, Y. Ma, H. Xiang, Y. Huang, *ACS Energy Lett.* **2022**, *8*, 372–380.
[86] J. Zheng, Q. Zhao, T. Tang, J. Yin, C. D. Quilty, G. D. Renderos, X. Liu, Y. Deng, L. Wang, D. C. Bock, C. Jaye, D. Zhang, E. S. Takeuchi, K. J. Takeuchi, A. C. Marschilok, L. A. Archer, *Science* **2019**, *366*, 645–648.
[87] M. Zhou, S. Guo, J. Li, X. Luo, Z. Liu, T. Zhang, X. Cao, M. Long, B. Lu, A. Pan, G. Fang, J. Zhou, S. Liang, *Adv. Mater.* **2021**, *33*, 2100187.
[88] X. Yang, W. Li, Z. Chen, M. Tian, J. Peng, J. Luo, Y. Su, Y. Zou, G. Weng, Y. Shao, S. Dou, J. Sun, *Angewandte Chemie International Edition* **2023**, *62*, e202218454.
[89] X. Li, Z. Chen, P. Ruan, X. Hu, B. Lu, X. Yuan, S. Tian, J. Zhou, *Nanoscale* **2024**, *16*, 2923–2930.
[90] W. Ge, H. Peng, J. Dong, G. Wang, L. Cui, W. Sun, X. Ma, J. Yang, *Chem. Commun.* **2024**, *60*, 750–753.
[91] X. Liang, X. Chen, Z. Zhai, R. Huang, T. Yu, S. Yin, *Chem. Eng. J.* **2024**, *480*, 148040.
[92] Q. Deng, S. You, W. Min, Y. Xu, W. Lin, J. Lu, C. Yang, *Advanced Materials* **2024**, *36*, 2312924.
[93] H. Zhang, Y. Zhong, J. Li, Y. Liao, J. Zeng, Y. Shen, L. Yuan, Z. Li, Y. Huang, *Adv. Energy Mater.* **2022**, *13*, 2203254.
[94] Y. Zou, X. Yang, L. Shen, Y. Su, Z. Chen, X. Gao, J. Zhou, J. Sun, *Energy Environ. Sci.* **2022**, *15*, 5017–5038.
[95] Q. Zhu, G. Sun, S. Qiao, D. Wang, Z. Cui, W. Zhang, J. Liu, *Adv. Mater.* **2024**, *36*, 2308577.
[96] Y. Wang, L. Mo, X. Zhang, Y. Ren, T. Wei, Z. Li, Y. Huang, H. Zhang, G. Cao, L. Hu, *Adv. Energy Mater.* **2023**, *13*, 2301517.
[97] J. Cao, D. Zhang, R. Chanajaree, Y. Yue, X. Zhang, X. Yang, C. Cheng, S. Li, J. Qin, J. Zhou, Z. Zeng, *ACS Appl. Mater. Interfaces* **2023**, *15*, 45045–45054.

Manuscript received: April 7, 2024
Revised manuscript received: May 20, 2024
Accepted manuscript online: May 20, 2024
Version of record online: July 3, 2024